Research Journal of Chemical Sciences ISSN 2231-606X
Vol. **5(12),** 88-97, December **(2015)** *Res. J. Chem. Sci.*

Development of Electrochemical Biosensor for the Detection of *Klebsiella pneumoniae* as Biological Weapon

Harish Kumar* **and Bhawana**
Material Science and Electrochemistry Lab., Dept. of Chemistry, Ch. Devi Lal University, Sirsa, Haryana, 125 055, INDIA

Available online at: www.isca.in, www.isca.me
Received 7th December 2015, revised 11th December 2015, accepted 17th December 2015

Abstract

Rapid, explicit detection and identification of Biological Warfare Agents (BWAs) with early warning signals for detecting possible biological attack is a main challenge for health, military and other government defence agencies. The current research is focussed on development of electrochemical biosensors for the detection of biological warfare agent. For this purpose, a carbon based (Graphene) working electrode containing enzyme alkaline phosphatase, cellulose acetate and Poly Vinyl Pyrolidone (PVP), Ferrocene, Horseradish peroxidase, aq. KOH was fabricated. It is then combined with Ag/AgCl reference and a platinum electrode (auxiliary) to form a three electrode based electrochemical biosensor for the electrochemical detection of Klebsiella pneumoniae as biological warfare agent in the presence and absence of Fe_3O_4 nanoparticles. Fe_3O_4 nanoparticles were produced by sol-gel technique and were characterized by UV-visible, FTIR, TEM and XRD techniques. Change in current response and OCP values helps in the detection of biological warfare agent in presence and absence of Fe_3O_4 nanoparticles. Effects of temperature, stirring and Fe_3O_4 nanoparticles on the BWA have also been investigated.

Keywords: Biological warfare agents, biosensors, Sol-gel method, Fe_3O_4 nanoparticles, *Klebsiella, pneumoniae.*

Introduction

The term Bioterrorism is defined as the use of a biological weapon (bacteria, virus or spores) on human life as a weapon of mass infection. It ultimately proves more powerful than a chemical or a nuclear weapon because it works silently and its effects can be extensive and out of control. List of pathogenic/harmful bacteria that may act as biological warfare agents is unending[1]. Highly dangerous include *Botulinum toxin, Francisellatularensis, Salmonella typhimurium, Staphylococcus epidermis, Klebsiella pneumoniae* and *Yersinia pestis*. Other bio-agents, like *Venezuelan equine encephalitis, Marburg, Ebola,* and influenza viruses are of lesser importance, despite the fact, that infections with these viruses are serious and mortality is relatively high, but due to the difficulty in their preparation, their position on the list of Biological Warfare Agents (BWA) is lower. First evidence of bioterrorism came in to existence in 1979, when doctors presented a report of mass civilian death due to B. anthracis pneumonia i.e. due to inhalation of anthrax. A person exposed to B. Anthracis died immediately. The bacilli of anthracis multiply rapidly in the body and produce a harmful toxin that stops the process of breathing.

On the other hand, Klebsiella pneumoniae can also be used as BWA. *K. pneumoniae* causes infection in lungs, where they cause necrosis, inflammation, and hemorrhage within the lung tissue. In comparison with chemical warfare agents (CWA), BWA production is much cheaper and terrorist or military attack with BWA is more effective in the range of hazard area and in the number of expected casualties. The infectious dose (ID) (amount of organism needed for infection outbreak) is different for every agent. Usually the intake of aerosol (particles 1 - 10 µm) through lung is able to evocate disease with a lower ID for the given BWA.

Different types of electrochemical biosensors which are in common practice are: Potentiometric, conductometric, amperometric, and impedimetric[2-5]. Out of these, amperometric biosensors are more common in practice and are typically based on the use of ion-selective working electrodes. These are three electrode based electrochemical systems which are attached with electrochemical detectors which measure the changes in analyte concentration during the course of reaction taking place at the surface of bio-recognition layer. The advantage of Amperometric biosensors over other biosensors is that they are highly sensitive, rapid, linear concentration dependent and inexpensive[6]. Amperometric biosensors aimed at microbial analysis have been reported by different researchers[7-11].

First biosensors used p*H* glass electrode with enzymes captured in a suitable membrane. In potentiometric immune-sensor electrochemical biosensor, enzyme-labelled antibodies are used. The most common labelling enzymes are urease, glucoseoxidase or alkaline phosphatase, which are able to change either p*H* or ionic strength in the course of the detection[12]. Very popular semiconductor-based biosensors are light-addressable potentiometric sensors (LAPS). Due to their small size and possible multichannel arrangement, these devices seem to be very convenient for simultaneous analysis of several analytes[13].

The LAPS immune-sensors were used to detect *Francisella tularensis*[14] with a limit of detection (LOD) at 3.4×10^3 cells/ml and *Bacillus melitensis* with LOD equal to 6×10^3 cells/ml during the 1h incubation time[15]. A better LOD was achieved for *Escherichia coli* DH5 a strain[16]; the secondary antibody specific against *Escherichia coli* labelled with urease was used and LOD of 10 cells/ml for1.5 h assay time was claimed.

In continuation to our earlier study[17], in this paper, we have focussed on the fabrication of electrochemical biosensor for the detection of *Klebsiella pneumoniae as* biological warfare agent.

Material and Methods

Samples of disease causing bacteria i.e. *Klebsiella pneumonia* (MTCC No. 3384) were collected on request from Microbial Type Culture Collection (MTCC), Institute of Microbial Technology, situated at Chandigarh, India.

Different steps used for the electrochemical determination of disease causing bacteria are:

Preparation of Bacterial Strain: The bacterial test organism *Klebsiella pneumonia* was grown in nutrient broth for 24.0 hours at 37.0 °C. Sodium phosphate buffer solution (pH 7.0) was selected to hold these disease causing bacteria at a very low temperature i.e. 4.0 ºC.

Synthesis of Fe_3O_4 Nanoparticles and Graphene: Fe_3O_4 nanoparticles were synthesized by Sol-gel technique. In this technique, metal salt solution having Ferric chloride is added drop wise in a mixture of tetraethyl orthosilicate in ethanol. Reduced graphene was synthesized by well known Hummers method.

Characterization of Fe_3O_4 Nanoparticles and Graphene: Characterization of Fe_3O_4 nanoparticles and Graphene were carried out by using UV-visible spectroscopy, Fourier Transform Infra-Red (FT-IR) technique, X-ray diffraction (XRD) study and Transmission Electron Microscopy (TEM) techniques.

Fabrication of Working Test Electrode: A carbon paste (Graphene) working electrode was fabricated for the electrochemical determination of biological weapon. A slurry was prepared by mixing reduced graphene, alkaline phosphatase, cellulose acetate, Ferrocene, Horseradish peroxidase, aq. KOH and Poly vinyl pyrolidone (PVP). This slurry was filled in working test electrode with the help of luggin capillary. A copper wire is dipped from outside in the slurry for making electrical connections.

Fabrication of Three electrodes based Electrochemical Cell: A three electrodes based electrochemical cell was fabricated having three electrodes i.e. a working test electrode (cellulose acetate, PVP bound carbon paste electrode), Ag/AgCl reference electrode and a platinum electrode acting as an auxiliary electrode for the electrochemical determination of disease causing pathogen (figure-1).

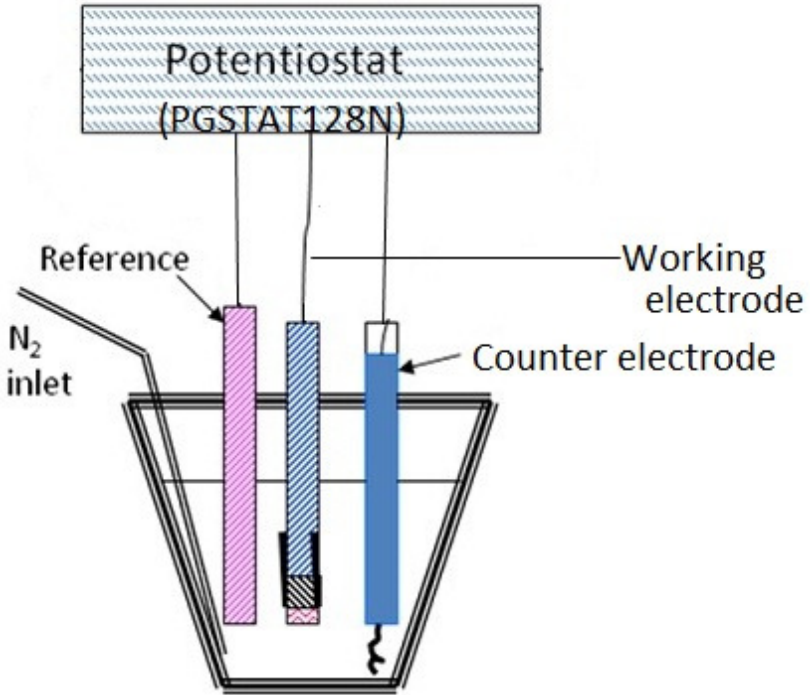

Figure-1
A three electrodes based electrochemical biosensor for the detection of biological warfare agent

Electrochemical Characterization: Three electrodes based electrochemical cell is connected to the instrument electrochemical workstation PGSTAT 128N, Metrohm Autolab attached to a PC and digital controlled water bath to maintain constant temperature. Electrochemical measurement experiments were performed on a pathogenic bacteria *Klebsiella pneumoniae* and change in Open Circuit Potential (OCP), current (nA) and potential values were recorded at different conditions.

For the electrochemical characterization, 3×10^7 CFU of *Klebsiella pneumoniae* in 50 ml of PBS buffer solution was used. Four different samples were prepared i.e. pure PBS buffer solution as sample 1, PBS buffer solution with 3×10^7 CFU of *Klebsiella pneumoniae* as sample 2, PBS buffer solution with Fe_3O_4 nanoparticles as sample 3 and PBS buffer solution with Fe_3O_4 nanoparticles and 3×10^7 CFU of *Klebsiella pneumoniae* as sample-4.

The above samples were kept under following two observations: Heating at a constant temperature of 70.0 ºC without stirring for 6.0 hours. Continuous stirring for 6.0 hours at room temperature.

After 6.0 hours, we have recorded the current and potential values with the help of three electrodes based electrochemical cell connected to the instrument PGSTAT 128N, Metrohm Autolab, Netherland.

Results and Discussion

Result of electrochemical characterization on *Klebsiella pneumoniae* is recorded in the form of tables-1 and 2 and figures-2 to 8. Table-1 shows OCP values of unstirred and after 6 hours of continuous stirring. Table-2 shows the OCP values of four heated samples at initial time and after 6.0 hours.

Figure-1 shows electrochemical biosensor for the detection of biological warfare agent. Figure-2 shows current and potential values of pure PBS buffer solution at 0.0 and 6.0 hours. Figure-3 shows current and potential behaviour of PBS buffer solution in presence of *Klebsiella pneumoniae* at 0.0 and 6.0 hours. Figure-4 shows current and potential behaviour of PBS buffer solution in presence of Fe_3O_4 nanoparticles (50 µl/ ml) at 0.0 and 6.0 hours. Figure-5 shows current and potential behaviour of PBS buffer solution in presence of *Klebsiella pneumoniae* and Fe_3O_4 nanoparticles (50 µl/ ml) at 0.0 and 6.0 hours.

Figure-6 shows current and potential values of pure PBS buffer solution at 0.0 and after 6.0 hours of heating at 70.0^0C. Figure-7 shows current and potential behaviour of PBS buffer solution in presence of *Klebsiella pneumoniae* at 0.0 and after 6.0 hours of heating at 70.0^0C. Figure-8 shows current and potential behaviour of PBS buffer solution in presence of *Klebsiella pneumoniae* and Fe_3O_4 nanoparticles (50 µl/ ml) at 0.0 and after 6.0 hours of heating at 70.0^0C.

Figure-9 shows UV-visible spectra of Fe_3O_4 metal nanoparticles synthesized by sol-gel technique as a function of wavelength. Figure-10 shows Fourier Transform Infra-Red (FT-IR) spectra (Thermo-USA, FTIR-3800) in the wavelength range of 400 - 4000 cm^{-1} of Fe_3O_4 nanoparticles produced by sol-gel technique. Figure-11 shows XRD pattern of Fe_3O_4 nanoparticles produced by sol-gel technique. Figure-12 shows TEM images of Fe_3O_4 metal nanoparticles produced by sol-gel technique.

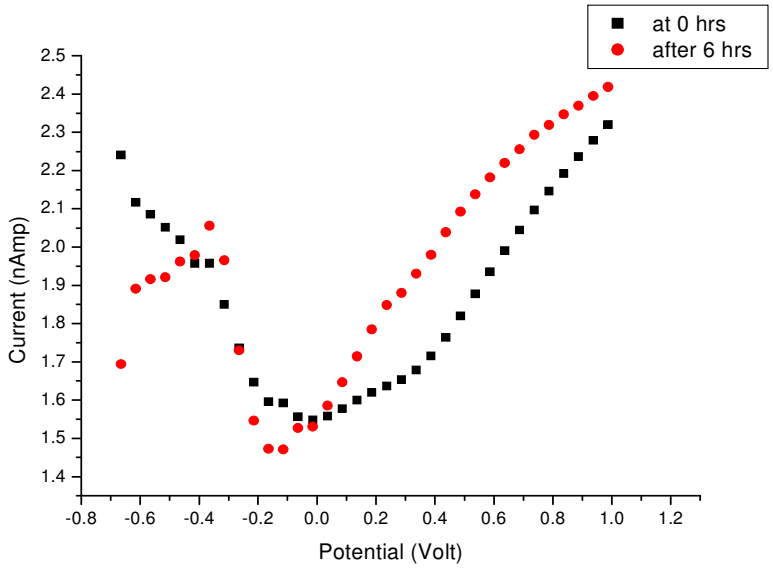

Figure-2
Current versus potential behaviour of pure PBS buffer solution at 0.0 and after 6.0 hours of stirring

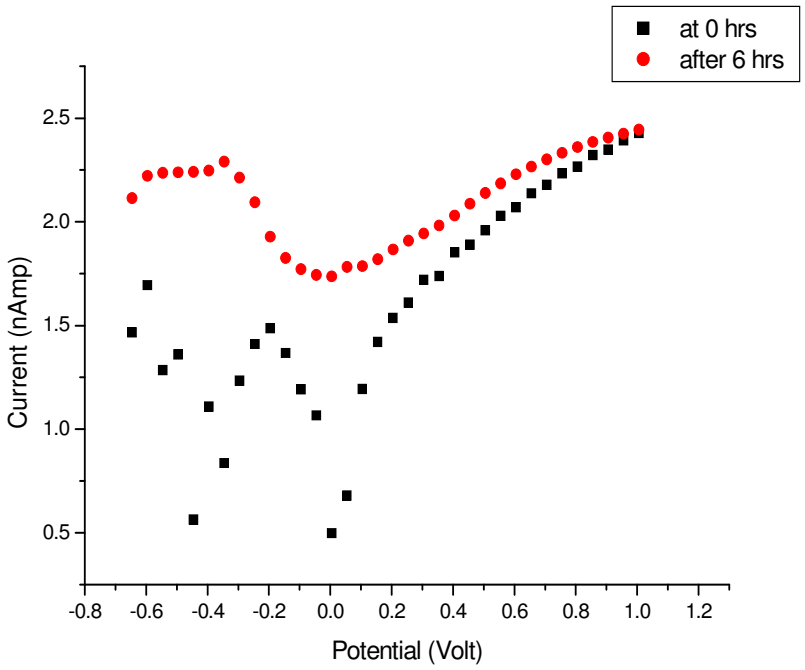

Figure-3
Current versus potential behaviour of PBS buffer solution in presence of Fe_3O_4 nanoparticles (50 µl/ ml) at 0.0 and after 6.0 hours of stirring

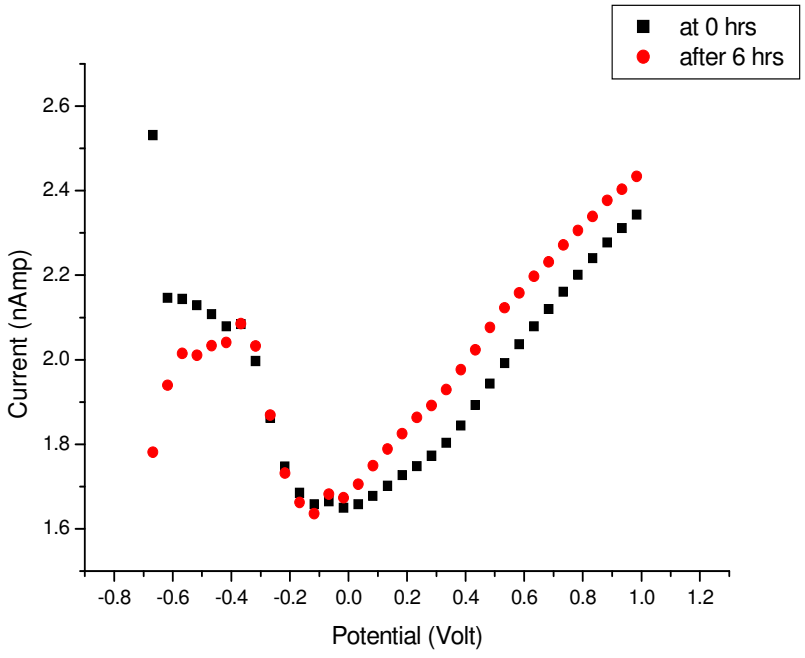

Figure-4
Current versus potential behaviour of PBS buffer solution with Klebsiella *Pneumoniae* at 0.0 and 6.0 hours of stirring

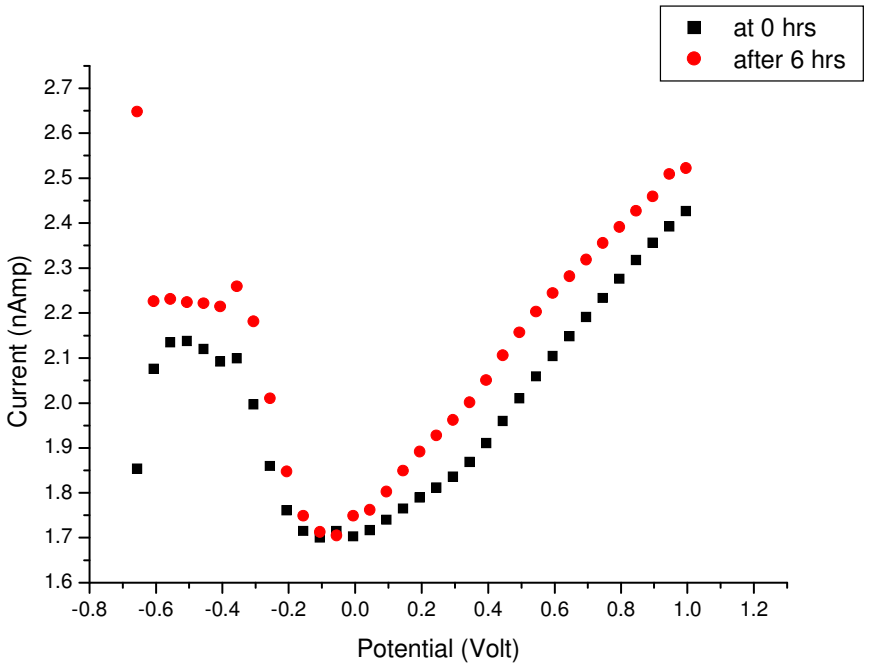

Figure-5
Current versus potential behaviour of PBS buffer solution in presence of Klebsiella *Pneumoniae* and Fe_3O_4 nanoparticles (50 µl/ ml) at 0.0 and 6.0 hours of stirring

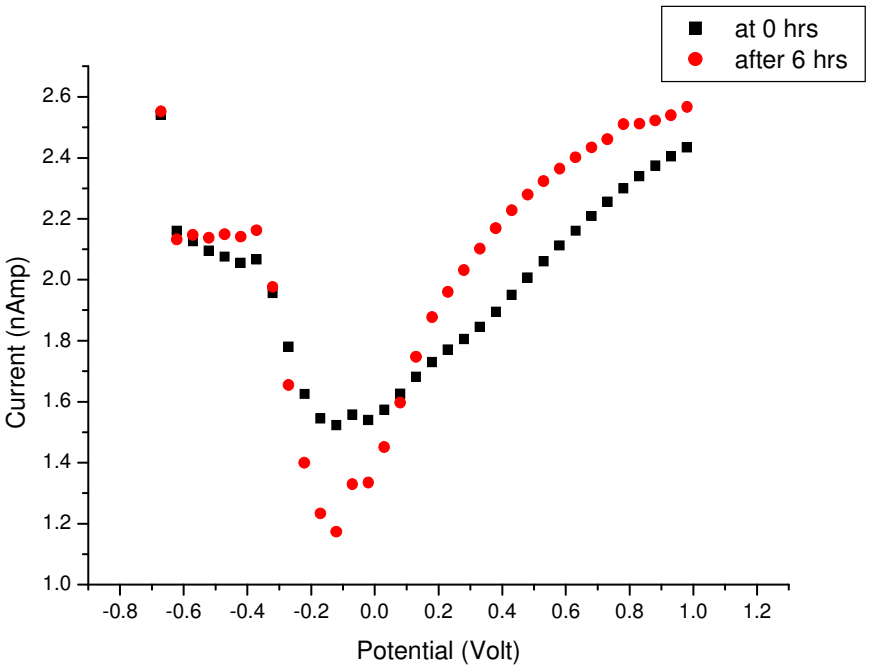

Figure-6
Current versus potential behaviour of pure PBS buffer solution at 0.0 and after 6.0 hours of heating

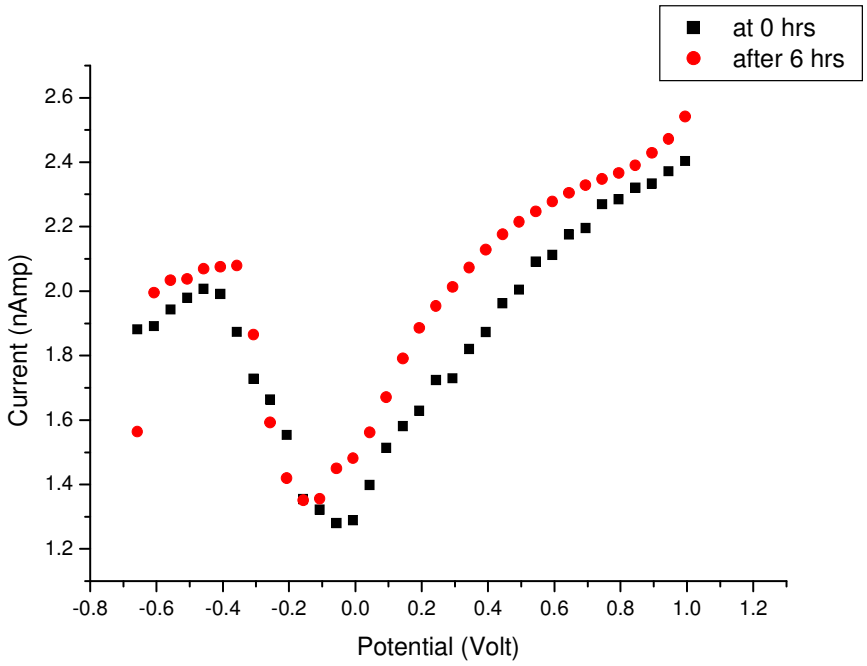

Figure-7
Current versus potential behaviour of PBS buffer solution in presence of Fe_3O_4 nanoparticles (50 µl/ ml) at 0.0 and after 6.0 hours of heating

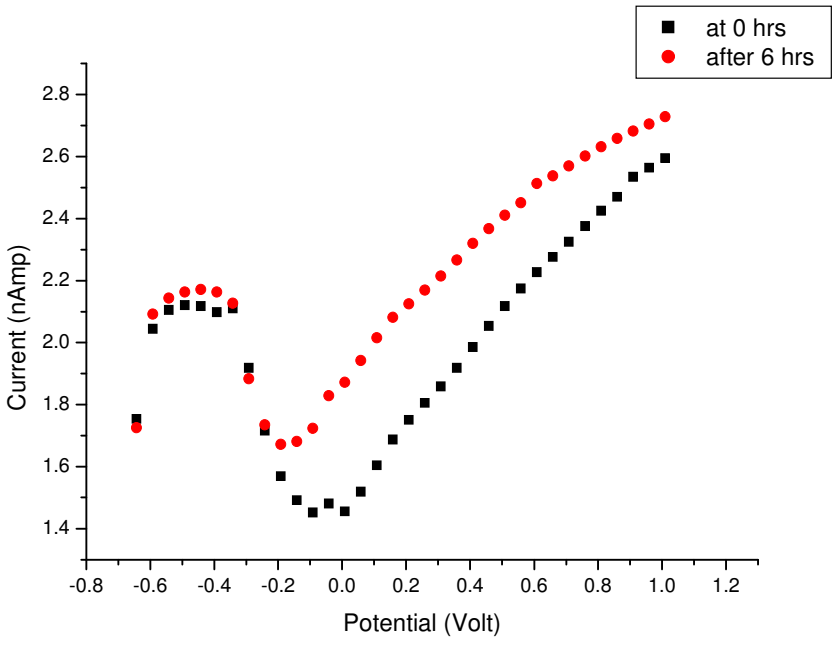

Figure-8
Current versus potential behaviour of PBS buffer solution in presence of Klebsiella *Pneumoniae* and Fe_3O_4 nanoparticles (50 µl/ ml) at 0.0 and after 6.0 hours of heating

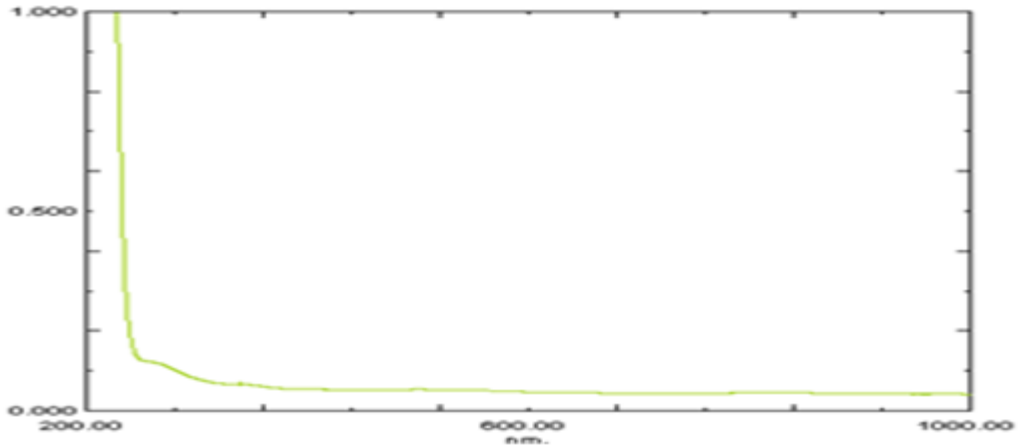

Figure-9
UV-Visible spectra of Fe_3O_4 nanoparticles

Discussion: The UV absorption band of Fe nanoparticles (figure-9) was observed in the wavelength range of 330–450 nm which may be due to the absorption and scattering of light by iron nanoparticles[18-19]. The low absorption band at a wavelength of 410 nm may be due to the formation of least agglomerated Fe_3O_4 nanoparticles. Absence of additional peaks corresponding to alcohol further indicates that the metal nanoparticles were not surrounded by ethanol and they only acted as a soft template.

FT-IR spectroscopic technique was carried out in order to ascertain the purity and nature of ferrite metal nanoparticles synthesized by sol-gel technique. A peak at 3,440 cm^{-1} in the FTIR spectrum of iron oxide nanoparticles (figure 10), proves traces of ferric hydroxide in Fe_3O_4[20-21]. The peaks at 565 and 421 cm^{-1} are may be due to the vibrations of Fe^{2+}–O^{2-} and Fe^{3+}–O^{2-} respectively[22]. Another peak (sharp and high intensity) at 565 cm^{-1} indicates the presence of crystallinity in the metal nanoparticles. The characteristic absorption bands at 565 and 421 cm^{-1} confirms the presence of spinel structure in Fe_3O_4 nanoparticles.

The reflection peak at $2\theta = 35.60^0$ confirm spinel phase of ferrite (Fe_3O_4) nanoparticles (JCPDS, PDF cards 3-864 and 22-1086) (figure-11). The diffractions peaks of the ferrite nanoparticles were observed at $2\theta = 30.18^0$ (d spacing = 0.297 nm), 35.61^0 (d spacing = 0.253 nm), 43.27^0 (d spacing = 0.209 nm), 53.56^0 (d spacing = 0.171 nm) and 57.11^0 (d spacing = 0.162 nm)[23]. The peaks at an angle of 30.18^0 (220), 35.612^0 (311), 43.278^0 (400), 53.569^0 (422), 57.118^0 (511) and 62.655^0 (440) correspond to Fe_3O_4. The average particle size of ferrite nanoparticles has been calculated using well known Scherrer equation[24] and was found to be 31.0 nm. Further, diffraction peak broadening confirms the formation of the fine Fe_3O_4 nanoparticles.

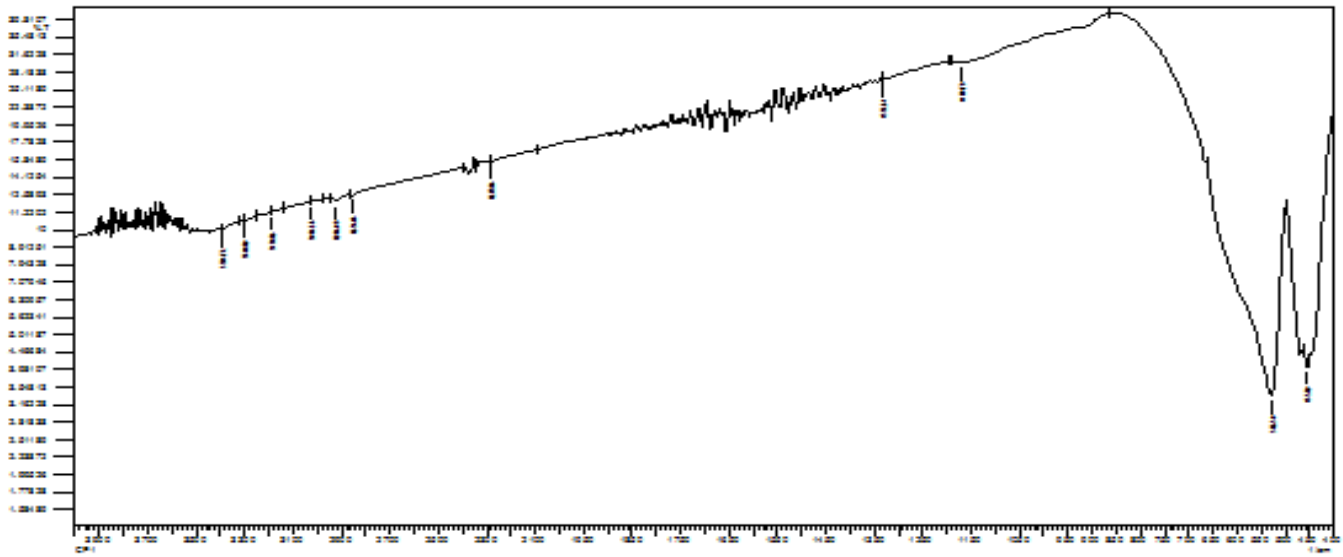

Figure-10
FT-IR spectra of Fe_3O_4 nanoparticles

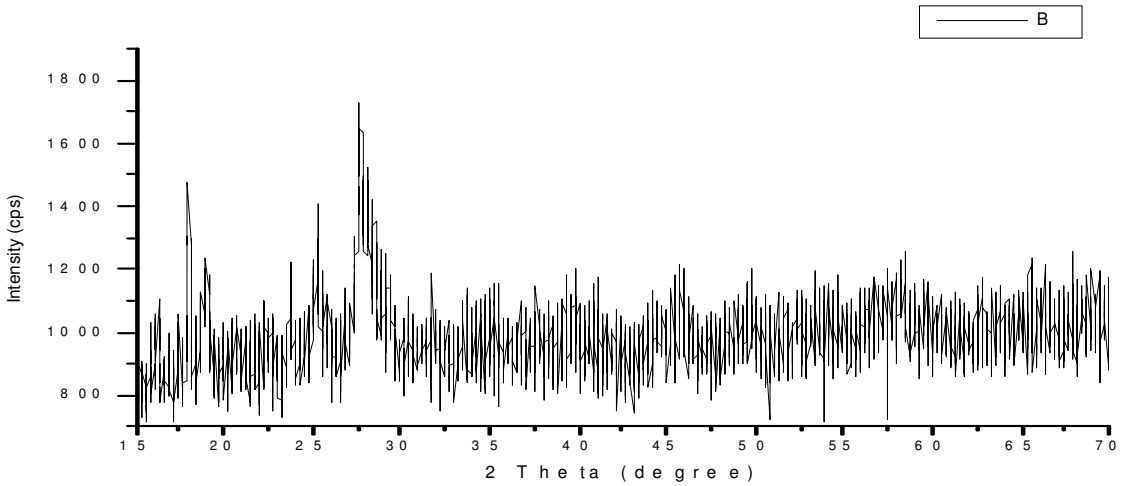

Figure-11
XRD diffraction pattern of Fe_3O_4 nanoparticles

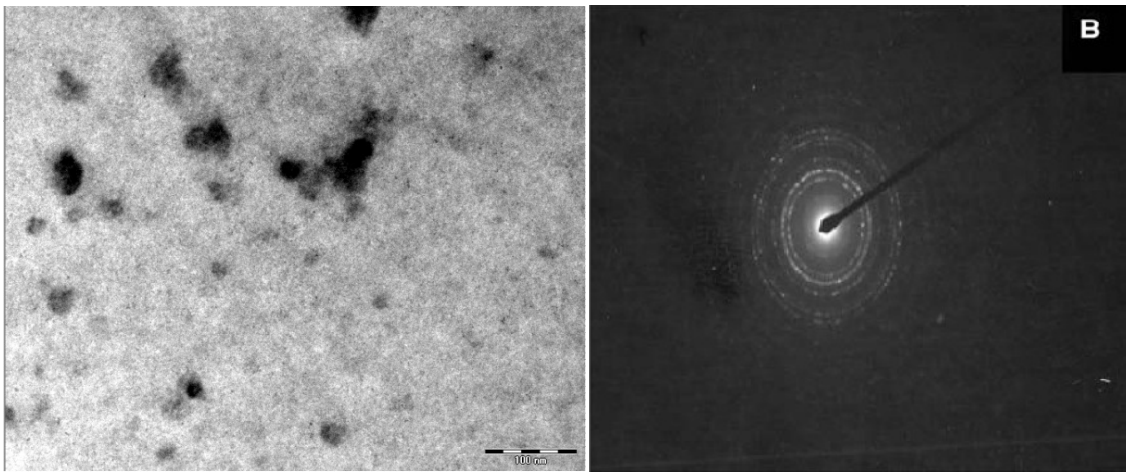

Figure-12
(a) TEM images of Fe_3O_4 nanoparticles (b) Diffraction pattern of Fe_3O_4 nanoparticles

Structural and optical properties of Fe_3O_4 nanoparticles were determined by using Transmission Electron Microscope (TEM) of made Morgagni 268 D, FEI Philips at a resolution of 2 A^0 from Electron Microscope Facility (SAIF), AIIMS, New Delhi (figure-12). The TEM images reveals self-organized network like morphology of ferrite (Fe_3O_4) nanoparticles which are almost identical in shape and found to be uniformly dispersed. The average particles size is in close agreement with both the technique i.e. as observed in TEM and the crystallite size calculated by the Scherrer equation (~31.0 nm) with the help of XRD technique. Further, the TEM diffraction ring (Figure 12 b) confirms that the ferrite nanoparticles are in a well crystalline state[25].

Purpose of addition of Horseradish peroxidase (HRP) in the slurry of working electrode is because HRP enhance the intensity of weak electrochemical signal. Ferrocene act as stimulator. Grapheme was added in to the slurry of working electrode in order to increase its conductivity and surface area of the electrode.

Table-1
OCP (Open Circuit Potential) values of stirred samples of Klebsiella pneumonia

Samples	**OCP Values (Volt) at 0.0 and 6.0 hours**	
Pure PBS solution	0.524	0.545
PBS solution with Fe_3O_4 nanoparticles	0.747	0.753
PBS solution with 3.0 $\times 10^7$ CFU of Klebsiella *Pneumoniae*	0.238	0.288
PBS solution with Fe_3O_4 nanoparticles and 3.0 $\times 10^7$ CFU of Klebsiella *Pneumoniae*	0.247	0.264

Table-2
OCP (Open Circuit Potential) values of heated samples of Klebsiella *Pneumoniae*

Samples	OCP Values (Volt) at 0.0 and 6.0 hours	
Pure PBS solution	0.514	0.553
PBS solution with Fe_3O_4 nanoparticles	0.782	0.550
PBS solution with 3.0×10^7 CFU of Klebsiella *Pneumoniae*	0.247	0.231

From the tables-1 and 2, it is observed that OCP value of PBS buffer solution decreases on addition of 3.0×10^7 CFU of *Klebsiella pneumoniae.* OCP value of PBS buffer solution increases on addition of Fe_3O_4 nanoparticles. OCP value of *Klebsiella pneumoniae* increases (0.238 to 0.247 V) on addition of Fe_3O_4 nanoparticles (50 µl/ ml). As Fe_3O_4 nanoparticles are electro active species and hence increase in OCP value is due to increase in electrical conductivity of the medium. Heating of sample no. 1 to 70.0^0C leads to increase in the OCP value from 0.514 to 0.553 V. Heating of sample no. 3 to 70.0 ^{0}C makes *Klebsiella pneumoniae* inactive which lowers its OCP value. It is observed from the table-1 that the addition of Fe_3O_4 nanoparticles (50 µl/ml) at room temperature in the sample containing 3.0×10^7 CFU of *Klebsiella pneumoniae* results into slight increase in OCP value.

It is observed from table-2 that heating of sample no. 3 to 70.0 ^{0}C for 6.0 hours results in decrease in the OCP value from 0.247 to 0.231 V. A constant OCP value of 0.247 V in phosphate buffer solution indicates the presence of *Klebsiella pneumoniae* pathogenic bacteria in the sample. Heating of the samples up to 70.0^0C for a definite period of time leads to decrease in OCP value. Addition of Fe_3O_4 nanoparticles leads to slight increase in OCP value i.e. heating of sample makes bacteria inactive which results in the decrease in OCP value.

It is observed from figure-2 that the current and potential behaviour of pure PBS solution remains almost same at 0.0 and 6.0 hours of continuous stirring. The current value first decreases and then increases with increase in potential value. It is observed from figure-3 that there is deviation in current value at smaller value of potential of PBS buffer solution in presence of Fe_3O_4 nanoparticles (50 µl/ ml) at 0.0 and after 6.0 hours of continuous stirring. But at higher potential value current and potential behaviour of pure PBS solution remains almost same. Current value increases on addition of Fe_3O_4 nanoparticles in phosphate buffer solution. Similar types of results were observed in case of samples containing *Klebsiella pneumonia* but deviation is small in comparison to Fe_3O_4 nanoparticles (figure-4). The current and potential behaviour of samples containing both Fe_3O_4 nanoparticles (50 µl/ ml) and 3.0×10^7 CFU of *Klebsiella pneumonia* are almost same at initial time and after 6.0 hours of continuous stirring (figure-5).

It is observed from the figure-6 that the value of current first decreases and then increases continuously with increase in potential value at initial time and after 6.0 hours of continuous stirring. It is observed from the figure-7 that the value of current first increase and then decrease and then increase with increase in potential value in presence of Fe_3O_4 nanoparticles at initial time and after 6.0 hours of heating at 70^0C. Figure 8 shows that value of current initially remains constant and then decrease and then continuously increase with increase in potential value in presence of 3.0×10^7 CFU of *Klebsiella pneumonia* in PBS solution at initial time and after 6.0 hours at a constant temperature of 70.0 ^{0}C. The current value increases slightly after six hours of heating at high value of potential.

Conclusion

A carbon (Graphene) based working electrode having alkaline phosphatase, cellulose acetate, Ferrocene, Horseradish peroxidase, aq. KOH and PVP was fabricated which when combined with Ag/AgCl reference and a platinum auxiliary electrode to form a three electrode based electrochemical cell for the electrochemical detection of *Klebsiella pneumoniae* as biological warfare agent. Fe_3O_4 nanoparticles were synthesized by sol-gel method. Characterization of Fe_3O_4 nanoparticles was carried out by using UV-visible, FT-IR, XRD and TEM techniques. An UV–visible absorption band at the wavelength of 410 nm and a sharp absorption band at 600 cm^{-1} in FTIR spectra confirm the formation of ferrite nanoparticles. OCP value of PBS buffer solution decreases on addition of 3.0×10^7 CFU of *Klebsiella pneumoniae.* OCP value of PBS buffer solution increases on addition of Fe_3O_4 nanoparticles. Current value increases on addition of Fe_3O_4 nanoparticles in phosphate buffer solution. A constant OCP value of 0.247 V in phosphate buffer solution indicates the presence of *Klebsiella pneumoniae* pathogenic bacteria in the sample.

Acknowledgement

Many-many thanks to Defence Research and Development Organisation (DRDO), New Delhi for providing us financial support for carrying out this research work.

References

1. North Atlantic Treaty Organization, NATO Handbook on the Medical Aspects of NBC Defensive Operations, Part II, Biological NATO Amed, **P-6(B)** (**1996**)

2. Karube I.; Hera K.; Matsuoka H. and Suzuki S., Amperometric determination of total cholesterol in serum with use of immobilized cholesterol esterase and cholesterol oxidase, *Anal. Chim. Acta*., **139**, 127 –32 (**1982**)

3. Veldhoven V.; Meyhi P.P. and Mannaerts G.P., Enzymatic quantitation of cholesterol esters in lipid extracts, *Anal. Biochem*, **258**, 152–55 (**1998**)

4. Shahnaz B., Tada S., Kajikawa T., Ishida T. and Kawanishi K., Automated fluorimetric determination of cellular cholesterol, *Ann. Clin. Biochem,* **345**, 665–70 (**1998**)

5. Kennedy J.F., In: Wiseman, A. (ed.) Handbook of Enzyme Biotechnology, Chap John Wiley and Sons, New York, (**1975**)

6. Singh S., Solanki P.R. and Malhotra B.D., Covalent immobilization of cholesterol esterase and cholesterol oxidase on polyaniline films for application to cholesterol biosensor, *Anal. Chim. Acta*., **568**, 126–32 (**2006**)

7. Kennedy J.F., Handbook of Enzyme Technology, Marcel Dekker, New York, (**1985**)

8. Lee W.E., Thomson H.G., Hall J.G., Fulton R.E. and Wong J.P., Characteristics of the Biochemical detector sensor, Defence Research Establishment Suffield, Canada, Suffield Memorandum No.1402, 1-23 (**1993**)

9. Ercole C., Del Gallo M., Pantalone M., Santucci S., Mosiello L., Laconi C. and Lepidi, *Sensor Actuators B*, **4163**, 1-5 (**2002**)

10. Ghindilis A.L., Atanasov P., Wilkins P. and Wilkins E.A., biosensor for *Escherichia coli* based on a potentiometric alternating biosensing (PAB) transducer, *Biosensors Bioelectronics*, **13**, 113-31 (**1998**)

11. Crowley E.L., O'Sullivan C.K. and Guilbault G.G., Increasing the sensitivity of listeria monocytogenes assays: Evaluating using ELISA and amperometric detection. Analyst, **124(3),** 295-99 (**1999**)

12. Mirhabibollahi B., Brooks J.L. and Kroll R.G., A semi-homogeneous amperometric immunosensor for protein A-bearing Staphylococcus aureus in foods, *Appl. Microbiol. Biotechnol*., **34**, 242 (**1990**)

13. Brooks J.L., Mirhabibollahi B. and Kroll R.G., Sensitive enzyme-amplified electrical immunoassay for protein A-bearing S. Aures in food, *Appl. Environ. Microbiol*., **56**, 3278-84 (**1990**)

14. Nakamura N., Shigematsu A. and Matsunaga T., Electrochemical detection of viable bacteria in urine and antibiotic selection, *Biosens. Bioelectron*, **6**, 575 (**1991**)

15. Brook J.L., Mirhabibollahi B. and Kroll R.G., Experimental enzyme linked immunosensor for the detection of Salmonella in food, *J. Appl. Bacteriology*, **73**, 189-96 **(1992)**

16. Kim H.J., Bennetto H.P. and Haqlablab M.A., A novel liposome based electrochemical biosensor for the detection of haemolytic microorganisms, *Biotechnol. Tech.,* **9(6),** 389-94 **(1995)**

17. Kumar H. and Rani R., Development of Biosensor for the detection of Biological Warfare Agents: Its Issues and Challenges, *Sci. Progress*, **96(3),** 294-308 **(2013)**

18. Koutzarova T., Kolev S., Ghelev C., Paneva D. and Nedkov I., Microstructural study and size control of iron oxide nanoparticles produced by microemulsion technique, *Phys. Stat. Sol.(c).*, **3(5),** 1302-07 **(2006)**

19. Bard X.J. and Faulkner L.R., Electrochemical Methods: Fundamentals and Applications, 2nd edn, Wiley, New York, **(2000)**

20. Chen X.; Wang Y., Zhou J., Yan W., Li X. and Hu J.J., Electrochemical impedance immunosensor based on three-dimensionally ordered macroporous gold film, *Anal. Chem.*, **80**, 2133-40 **(2008)**

21. Meng J.H., Yang G.Q., Yan L.M. and Wang X.Y., Synthesis and characterization of magnetic nanometer pigment Fe_3O_4, *Dye. Pigments*, **66**, 109-13 **(2005)**

22. Kaushik A., Khan R., Solanki P.R., Pandey P., Alam J., Ahmad S. and Malhotra B.D., Iron oxide nanoparticles-chitosan composite based glucose biosensor, *Biosens. Bioelectron*, **24(4),** 676-83 **(2008)**

23. Boistelle R. and Astier J.P., Crystallization mechanism in solutions, *J. Cryst. Growth*, **90**, 14-30 **(1988)**

24. Moudgil H.K., A textbook of Physical Chemistry, 2nd Edn., Prentice Hall of India, Pvt. Ltd., New Delhi, 648-50 **(2015)**

25. Wang J., Chen Q., Zheng C. and Hou B., Magnetic-field-induced growth of single-crystalline Fe_3O_4 nanowires, *Adv. Mater*., **16**(2), 137-40 **(2004)**